A program for real-time surveillance of SARS-CoV-2 genetics

Hayden N. Brochu[1], Kuncheng Song[1], Qimin Zhang[1], Qiandong Zeng[1], Adib Shafi[1], Matthew Robinson[1], Jake Humphrey[1], Bobbi Croy[2], Lydia Peavy[3], Minoli Perera[3], Scott Parker[3], John Pruitt[3], Jason Munroe[4], Rama Ghatti[5], Thomas J. Urban[3], Ayla B. Harris[3], David Alfego[1], Brian Norvell[3], Jonathan D. Williams[3], Deborah Boles[3], Melinda B. Nye[6], Suzanne E. Dale[6], Michael Sapeta[6], Christos J. Petropoulos[7], Jonathan Meltzer[6], Marcia Eisenberg[3], Oren Cohen[8], Stanley Letovsky[1], & Lakshmanan K. Iyer[1,*]

*[1]Labcorp Center for Excellence in Data Science, AI and Bioinformatics, Burlington, NC 27215, USA; [2]Labcorp Information Technology, Burlington, NC 27215, USA; [3]Labcorp Research and Development, Burlington, NC 27215, USA; [4]Labcorp Consumer Genetics Department, Burlington, NC 27215, USA; [5]Labcorp-Sequenom, San Diego, CA 92121, USA; [6]Labcorp Center for Esoteric Testing, Burlington, NC 27215, USA; [7]Labcorp-Monogram Biosciences, South San Francisco, CA 94080, USA; [8]Fortrea Inc., Durham, NC 27703, USA; *Corresponding author*

Please direct all correspondence to Lakshmanan K. Iyer (iyerl@labcorp.com)

A program for real-time surveillance of SARS-CoV-2 genetics

Abstract

The COVID-19 pandemic brought forth an urgent need for widespread genomic surveillance for rapid detection and monitoring of emerging SARS-CoV-2 variants. It necessitated design, development, and deployment of a nationwide infrastructure designed for sequestration, consolidation, and characterization of patient samples that disseminates de-identified information to public authorities in tight turnaround times. Here, we describe our development of such an infrastructure, which sequenced 594,832 high coverage SARS-CoV-2 genomes from isolates we collected in the U.S. from March 13th 2020 to July 3rd 2023. Our sequencing protocol ('Virseq') generates mutation-resistant sequencing of the entire SARS-CoV-2 genome, capturing all major lineages. We also characterize 379 clinically relevant SARS-CoV-2 multi-strain co-infections and ensure robust detection of emerging lineages via simulation. The modular infrastructure, sequencing, and analysis capabilities we describe support the U.S. Centers for Disease Control national surveillance program and serve as a model for rapid response to emerging pandemics at a national scale.

Introduction

The rapid emergence of COVID-19 and looming burden on global healthcare systems warranted swift responses from the international community. The causal virus, SARS-CoV-2, was first identified by metagenomic RNA sequencing[1] as well as Sanger- and PCR-based detection methods[2,3]. Very early in the pandemic response, we prioritized the development of SARS-CoV-2 diagnostic assays to meet the demand for detection methods, offering one of the first PCR-based tests and performing as many as 275,000 tests daily[4]. This immense scale of PCR testing enabled

us to assess the dynamics of COVID-19 infection as it pertains to PCR positivity[5] and also provide population-based analysis on the maintenance of antibody titers[6,7].

Similar to other betacoronaviruses, the SARS-CoV-2 genome mutated as it infected and spread across the population, with a mutation rate of approximately 1-2 x 10^{-6} mutations per nucleotide per replication cycle[8]. Such genetic changes are known to impact the severity and transmissibility of infection as well as vaccine efficacy[9], thus requiring close to real-time surveillance using next generation sequencing (NGS)-based methods to inform public health policies. Multiple whole genome sequencing approaches have been applied to support this need, namely the ARTIC SARS-CoV-2 amplicon-based protocol for whole genome sequencing[10], direct RNA sequencing[11], and sequence hybridization[12]. Shotgun metagenomic sequencing of wastewater has also been an effective surveillance strategy for approximating variant abundances[13] and identifying so-called 'cryptic lineages'[14,15], as it became apparent that COVID-19 patients exhibit fecal viral shedding[16,17].

Ultimately, a greater need for high-throughput, real-time genomic sequencing of SARS-CoV-2 emerged in the United States through the SARS-CoV-2 Sequencing for Public Health Emergency Response, Epidemiology and Surveillance (SPHERES) spearheaded by the Centers for Disease Control (CDC). To address this public health need and in collaboration with CDC SPHERES, we rapidly developed a national surveillance apparatus using our purposely designed infrastructure for flexible sampling, a unique approach for SARS-CoV-2 whole genome sequencing, and tailored analytical methodologies that ensure continuously robust SARS-CoV-2 lineage determination using the Phylogenetic Assignment of Named Global Outbreak (PANGO) nomenclature[18]. Our assay, which we call 'Virseq', is distinguished from other NGS-based SARS-CoV-2 whole genome sequencing approaches through its use of probe-based tiling[19] and long

reads, which provide versatile, mutation-resistant capabilities. As of July 3rd, 2023, we have sequenced 594,832 genomes (10X median depth of coverage) and have provided 524,498 high-quality SARS-CoV-2 genomes (10X median depth of coverage, >90% genome coverage, complete S gene coverage) and patient demographic data to the CDC using our Virseq assay, representing continuous snapshots of SARS-CoV-2 viral evolution.

In this study, we provide a retrospective analysis of our Virseq assay using our vast repertoire of high-quality genomes, showcasing our surveillance capabilities and the modular resources that support its continued use. We show that Virseq has generated uninterrupted surveillance reflecting the nationwide prevalence of SARS-CoV-2 consistent with our RT-PCR sample collection, and we further demonstrate the robustness of SARS-CoV-2 lineage determination through our in-house analytical capabilities. We also address the analytical challenges posed by rare SARS-CoV-2 co-infections by developing a custom workflow that yields haplotype-resolved consensus genomes. Finally, we pose this suite of resources as a model for mounting rapid and robust large-scale surveillance networks.

Results

An infrastructure for nationwide COVID-19 surveillance

The rapid emergence and continuous evolution of SARS-CoV-2 necessitated setting up a national surveillance program that could provide real-time epidemiological snapshots across the United States. In response to the CDC's basal surveillance program, we organized and implemented a nationwide infrastructure to identify SARS-CoV-2 positive patient samples across the United States, consolidate these samples and their associated demographic data, and sequence their genomes to determine their SARS-CoV-2 PANGO lineages. Our surveillance system also includes

68 mechanisms for monitoring emerging lineages and their potential impacts on qPCR and
69 sequencing performance. Further, this setup is flexible and modular, enabling rapid responses and
70 developments to our pathogen surveillance.

71 A schematic of this modular infrastructure and its associated sequencing protocols is shown
72 in **Figure 1**. In **Figure 1a**, we show a high-level view of our surveillance pipeline that begins with
73 sample accessioning and resulting in whole genome sequencing reports with de-identified sample
74 metadata. Upper respiratory samples (nasopharyngeal (NP) or nasal swabs) collected in 0.9%
75 saline or viral transport media were collected and analyzed through our COVID-19 RT-PCR Test
76 at various Labcorp® service centers and laboratories, and the resulting PCR extraction plates
77 containing SARS-CoV-2-positive samples were then shipped to Labcorp® central locations and
78 consolidated into plates with high viral titer samples (i.e. N1 Ct < 31) using our custom developed
79 plate selector app (**Figure 1b**, Methods). The selection of plates using this app is critical, as it de-
80 identifies data thereby ensuring HIPPA compliance and allows flexibility in choosing samples. For
81 example, we can focus on certain geographic regions where outbreaks are underway, put
82 limitations on the amount of data from a state to ensure uniform surveillance, and threshold on the
83 PCR amplification N1 Ct value to ensure sufficient genetic material is available for sequencing in
84 each sample. The resulting consolidated plates of high viral titer samples were then shipped to our
85 sequencing labs where samples were processed through custom tiled Molecular Loop® probe
86 amplification, followed by library preparation and sequencing on the PacBio® Sequel II™ platform
87 in a highly multiplexed fashion (**Figure 1c-d**). PacBio® raw data was then processed to generate
88 Circular Consensus Sequencing (CCS) reads which were then analyzed using our custom
89 bioinformatics workflow to generate consensus genomes for each sample (**Figure 1d**). Stringent
90 sequence coverage quality control was then applied followed by PANGO lineage determination

91 for each sample (Methods), and results were then merged with patient demographic data and de-
92 identified with a new custom ID generated for each sample (**Figure 1d**). Consensus genomes,
93 summary reports, raw CCS reads, and alignment variant calls were then provided to CDC who in
94 turn processed our submission and deposited the relevant data to public repositories, namely
95 GISAID[20] and NCBI[21].

96 ***High-throughput, high-fidelity SARS-CoV-2 genome surveillance pipeline***

97 The rapid pathogen evolution during a pandemic and the possibility of sporadic outbreaks
98 necessitates a highly robust genomic surveillance pipeline. From January 2021 to July 2023, we
99 have used our Virseq pipeline (**Figure 1**) to report 524,498 high-quality SARS-CoV-2 genomes
100 (10X median depth of coverage, >90% genome coverage, complete S gene coverage) and patient
101 demographic data to the CDC. These sequences captured all major lineages that have emerged
102 throughout the COVID-19 pandemic since the inception of this surveillance effort, including
103 Alpha, Delta, Omicron, and the many Omicron subvariants (**Figure 2**, Methods). When overlaying
104 the positivity rate of our diagnostic PCR assays used for sample picking, we observed multiple
105 fluctuations matching variant emerges, such as BA.1, BA.4/BA.5, and XBB.1.5 (**Figure 2b**).
106 Stratifying genomes by U.S. Health and Human Services (HHS) region (HHS regions 1-10;
107 Methods), we found that the HHS regions 1 and 2 (corresponding to the U.S. Northeast) often
108 served as a harbinger to predict variant emergence for all other regions (**Figure S1**). For example,
109 the initial Omicron variant (BA.1) and the more recent XBB.1.5 variant reached ~50% prevalence
110 in HHS regions 1 and 2 approximately one week and four weeks prior to all other regions,
111 respectively (**Figures S1 and S2**).

112 After the BA.1 wave, reports indicated that SARS-CoV-2 infections by Omicron variants
113 exhibited lower viral loads[22,23], prompting us to investigate the diagnostic PCR N1 Ct values of

our samples, which are a useful proxy for viral load. As expected, lower sample Ct values were correlated with both increased average depth of coverage and higher consensus genome coverage (**Figure S3a**). We also observed shifts in sample diagnostic N1 Ct values throughout the pandemic that ranged from 20-21 in 2021 and exceeded 24 during the BA.1 wave in the 2021-2022 winter season, prior to reaching a steady state between 22-23. (**Figure S3b**). In our later analysis of SARS-CoV-2 co-infections, we found that co-infected sample N1 Ct values followed the same trends as those of samples where only a single SARS-CoV-2 lineage was detected. Together, these results indicate that our surveillance captures the overall kinetics and patterns of circulating variants.

This collection of high-quality genomes also uniquely captured demographic trends from all 50 states in the U.S. and the District of Columbia. States with the highest representation include California (n>62,000) and New Jersey (n>48,000), while other key states from HHS regions 9 and 10 (WA, n >19,000; AZ, n>17,000), HHS region 5 (IL, n>23,000; OH, n>10,000), and HHS regions 4 and 6 (NC, n>45,000; FL, n>36,000; TX, n>14,000) also had strong sampling (**Figure 3a**, **Table S1**). We also observed that the number of Virseq-generated genomes has represented a consistent proportion of total SARS-CoV-2-positive samples collected in each HHS region with minor fluctuations (**Figure 3b**). These fluctuations are expected as the timing of variant outbreaks (e.g. BA.1) can vary across HHS regions along with concomitant surges in PCR positivity rate (**Figure 2b**). Despite these changes, we still observed sustained census normalized sampling across both our diagnostic PCR assays and Virseq (**Figure S4a**) even with an end to the COVID-19 emergency response and the reduction in our surveillance volume in 2023 (**Figure S4b**). Notably, we observed a reduction in Virseq surveillance in HHS regions 6-8 at the onset of the BA.2 wave, as BA.2 prevalence spiked elsewhere in the U.S. before affecting these regions (February 2022; **Figures 2b, 3b**, **S1, S2, and S4**).

We also found that the age distribution of samples collected in each geographic region shifted throughout the course of the pandemic, with a plurality from pediatrics in 2021, shifting to a more even distribution of ages in 2022, and finally shifting to a plurality from older segments of the population in 2023 (**Figures S5 and S6**). Interestingly, there was also a modest trend in patient-reported gender, as the proportion of samples from female patients appeared to increase from 2021 to 2022 and once again in 2023 (**Figures S5 and S6**), despite there not being any difference in PCR positivity between males and females (**Figure S7a**). We also observed a bifurcation in PCR positivity across age groups in March 2022, as pediatric PCR positivity lowered to approximately half of the positivity in most other age groups and this relative difference has not changed since (**Figure S7b**). Intriguingly, two months prior (January 2022), the CDC and FDA announced multiple expansions of pediatric COVID-19 vaccination availability[24–26] (**Figure S7b**). We also observed that in June 2022, 18–19-year-olds had a reduction in PCR positivity relative to older age groups as well, and most recently in June 2023 we observed an increase in geriatric (80+ year olds) PCR positivity (**Figure S7b**). These demographic- and region-specific trends in variant prevalences and PCR positivity rates require a surveillance apparatus like ours that is flexible and robust to the rapid evolution of the SARS-CoV-2 genome.

Robust, mutation-resistant S gene sequencing using a probe-based long-read strategy

To maintain nationwide surveillance of pathogen genome evolution, the selected whole-genome sequencing approach must be able to withstand sudden changes in genetic diversity. Our surveillance apparatus uniquely employs a probe-based long-read sequencing approach that is mutation-resistant by design due to its ~22X genome tiling of >99% of the SARS-CoV-2 genome, except for a few hundred base pairs of the 5'- and 3' peripheral genomic regions (**Figure 1c**). At the end of 2021, the Omicron variant (BA.1) emerged and swept through the U.S. in a matter of

160 weeks (**Figures 2**, **S1, and S2**), dramatically shifting the diversity of the circulating lineages across
161 the U.S. population (**Figure 4a**). Unlike earlier variants like Delta which were predominantly
162 mutated in the ORF1a genic region, the original Omicron variant (BA.1) introduced a surge of
163 novel S gene mutations (27 SNPs and three deletions compared to Delta) (**Figure 4b**), raising
164 concern regarding the ability of PCR- and amplicon-based assays to detect BA.1. In fact, the Spike
165 gene target failure (SGTF) genomic signature was so common that it became a useful proxy for
166 the PCR detection of emerging variants, such as Alpha and Omicron[27]. While interruptions in our
167 surveillance were not observed (**Figure 2**), we verified the fidelity of our sequencing of BA.1*
168 using an *in silico* approach to check for probe dropout caused by lineage defining mutations
169 (Methods). We found that our assay retained ~20X *in-silico* tiling of the S gene during the initial
170 Omicron wave (**Figure 4c**), and in the worst-case scenario where we allowed zero SNP tolerance
171 in probe binding regions, we retained a minimum of ~10X probe tiling (**Figure S8**). Furthermore,
172 as the total number of unique mutations and the concurrent prevalence of multiple circulating
173 lineages measured in terms of their entropy continues to increase with more recent XBB
174 subvariants, we continue to observe profoundly stable genome-wide probe tiling *in silico* (**Figure**
175 **4c**). This robust probe tiling is especially important as chronic infections and widespread
176 vaccination have altered the evolutionary trajectory of the SARS-CoV-2 genome[28] and the receptor
177 binding domain of the S gene remains under considerable selective pressure in the Omicron era[8].
178 We also confirmed the robustness of our sequencing strategy by analyzing the genome-
179 wide per-base coverage of Variants of Concern (VOCs) that have emerged throughout the
180 pandemic (**Figure S9**, starting with B.1.1.7 or 'Alpha' up until XBB.1.5). We found that overall
181 per-base coverage has remained stable and well above our minimum per-base coverage required
182 for base calling in our consensus genomes, despite the heavily mutated S gene of Omicron and

183 subvariants thereof (**Figure S9**). Together, these results show that the Virseq assay is a stable and
184 effective sequencing strategy and is a critical component of our surveillance apparatus. However,
185 while we are confident in our response to variant outbreaks thus far, it is imperative that proactive
186 measures are taken to preclude future surveillance interruptions.

187 ***Modeling the performance of the Virseq assay by simulation***

188 One challenge of sustaining continuous whole genome surveillance is the need to predict changes
189 in sequencing performance that may occur and its effect on the characterization of the pathogen
190 variants. Many SARS-CoV-2 lineages emerge in regions outside of our surveillance network (i.e.
191 in countries other than U.S.) and may be too rare for detection once they initially spread to our
192 surveilled regions. To address this challenge, we developed a Virseq performance simulator that
193 models our entire production process from raw reads to PANGO lineage determination, capturing
194 the sequencing and other systematic errors that might propagate into consensus genomes. This
195 simulator was constructed using a representative batch of samples and incorporates the per-base
196 coverage and minor allele fractions commonly observed at each genomic position (Methods,
197 **Figure S10**). Application of this simulator begins with an input sequence that is then mutated to
198 reflect any errors introduced by our production process, which can then be compared with the
199 original sequence via concordance analysis of their PANGO lineage determinations.

200 We routinely use this simulator to monitor newly designated lineages in the PANGO
201 nomenclature (largely VOCs) as well as randomly selected sequences from previous months of
202 surveillance, leveraging the GISAID database[20]. This routine monitoring mechanism is a crucial
203 component of our FDA EUA and could be used to help maintain future pandemic surveillance
204 networks. In this study, we expanded this analysis to include up to 100 sequences each from 1,899
205 VOCs (97,421 total sequences, 'VOC experiment') and descendant lineages thereof, current and

former, and 10,000 randomly selected sequences from each month spanning from January 2021 until July 2023 (310,000 total sequences, 'retrospective experiment') (Methods). As expected, we observed similar coverage profiles between the two experiments and the simulator model, indicating that the simulated genomes accurately reflected Virseq-generated sequences (**Figure S10b**). When assessing the PANGO lineage concordance between the simulated and original genomes, we first checked for exact matches then also checked for parent/child relationships between the lineages compared (e.g. BA.5 is a parent of the child BA.5.1), deeming these parent matches (Methods).

Overall, we observed strong concordance in both the retrospective (99.55% exact, 99.97% parent) and VOC experiments (99.06% exact, 99.84% parent) (**Figure 5**). In the retrospective experiment we observed strong concordance across all 31 months analyzed with some month-to-month fluctuations (>98.95% exact, >99.9% parent) (**Figure 5a**). We also observed that some fluctuations coincided with shifts in circulating lineage diversity and the timing of VOC emergences (**Figure 4**, **Figure 5a**). Intriguingly, while some VOC emergences resulted in slight reductions of concordance (BA.1, BA.4/BA.5), others counterintuitively coincided with improved concordance (BA.2, BQ, XBB.1.9/XBB.1.16) (**Figure 4**, **Figure 5a**).

When assessing the concordance of individual VOCs, we found that 98.21% (1,865) and 99.63% (1,892) of VOCs had >90% exact and parent lineage concordance, respectively (**Figure 5b**). In total, we observed seven VOCs with a small number of discordant calls, and four of these (BA.2.2.1, BA.5.10, BQ.1.19, and BY.1) had UShER tree placement conflicts with their designated hashes, i.e. these sequences were representative of those lineages but could not be placed accordingly in the UShER tree (**Table 1**). This indicated that the original sequences of these VOCs had unstable PANGO lineage designations. For example, one of four simulated BA.2.2.1

229 sequences was called a BA.1, and we later found that the original sequence was hashed as BA.2.2.1
230 but placed in the UShER tree as BA.1 (**Table 1**). Inspection of the other three VOCs revealed that
231 they were recombinants with discordant calls corresponding to one of the recombined lineages
232 (**Table 1**), indicating that the simulated genomes had a loss of resolution.

233 We then investigated features of the simulated genomes, including key drivers of
234 discordant lineage calls. As expected, we found that genome coverage was significantly lower
235 among genomes that had discordant lineage calls or that were only parent concordant compared to
236 those with exact concordance in both experiments ($p<0.001$ in all comparisons, Wilcoxon rank-
237 sum test, **Figure S11a-b**). Both experiments yielded similar genomic positional dependence of
238 consensus genome errors (**Figure S11c**), and these errors were often found in regions modeled
239 with poor coverage (5'/3' peripheral genomic regions) instead of positions modeled with higher
240 base calling errors (**Figure S11d-e**). These simulation experiments collectively show that the
241 Virseq assay generates consensus genomes with accurate PANGO lineage designations and that
242 accuracy is predominantly driven by genomic coverage, which is expected behavior for the
243 pangolin software in general[29]. This Virseq simulator is a crucial component of our surveillance
244 apparatus, ensuring that we anticipate potential sequencing interruptions and serving as a model
245 for viral sequencing simulators in general.

246 ***Detection and haplotype phasing of SARS-CoV-2 mixtures***

247 The concurrent circulation of multiple lineages of the same virus during a pandemic may result in
248 co-infections of different viral lineages, which in some cases result in more severe clinical
249 outcomes in COVID-19 patients[30]. Thus, another requirement for effective surveillance machinery
250 is the ability to distinguish and characterize co-infections, which may complicate consensus
251 genome generation and PANGO lineage determination. After an initial finding of within-host

252 SARS-CoV-2 diversity[31], reports emerged describing patients likely co-infected with co-
253 circulating SARS-CoV-2 lineages[32–37]. Since our SARS-CoV-2 whole genome sequencing dataset
254 robustly captures these pandemic-wide trends in circulating lineages (**Figure 2**) and is highly
255 stable (**Figure 4**, **Figure 5**), we posited that recovery of multiple SARS-CoV-2 lineage detections
256 from the same sample would be possible.

257 To identify these potential mixtures (i.e. co-infections), we developed a custom workflow
258 utilizing freyja[14], an off-the-shelf mixture deconvolution algorithm (Methods). We found that
259 deeply sequenced samples (20.7% or 123,373 of 594,832) produced stable lineage mixture results
260 (>99% genome coverage, 100% S gene coverage, and average depth of coverage > 200X) (**Figure**
261 **S12a**). We then imposed three criteria for a sample to be classified as a mixture. The first two
262 require the most and second most abundant lineages to have relative abundances no greater than
263 0.8 and no less than 0.2, respectively, which only 571 (0.46% of 123,373) samples satisfied (**Figure**
264 **S12b-c**). Thirdly, we required the mixed lineages to differ by at least three defining SNPs
265 (heretofore defined as 'discriminating SNPs'), since such mixtures were found to have stronger
266 concordance between lineage relative abundances and discriminating SNP allele fractions **Figure**
267 **S12d-f**). This process yielded a final confident set of 379 mixtures (**Supplementary Data**) likely
268 of similar quality to their non-mixture counterparts, as they were found to have similar median
269 depth of coverage (mixtures: 338.4, non-mixtures: 335.6, p=0.46, Wilcoxon rank-sum test)
270 (**Figure S12g**). These mixtures had similar Ct values as non-mixtures, with the same differences
271 observed between the BA.1 wave samples and those before and afterwards (**Figure S3c**). We also
272 found that these mixtures had lineage compositions concordant with the original lineage called by
273 pangolin[29], since in most cases the pangolin-derived lineage either closely matched the majority

274 mixture lineage (217 or 57.3%) or was a parent of both majority and minority mixture lineages
275 (142 or 37.5%) (**Figure S13**).

276 Not surprisingly, we detected a plurality of mixtures during the BA.1 wave (159 or 42%),
277 which represents the largest portion of the dataset analyzed (18% or 22,169 samples). We also
278 observed the highest prevalence of mixtures during the BA.1 wave, peaking at 1.4% the last week
279 of December 2021 (**Figure 6a**). When categorizing the lineages comprised by these mixtures using
280 their lineage groups, we found that most mixtures were of lineages from the same group (347 or
281 91.6%), e.g. BA.1* mixed with BA.1* (**Figure 6b**, **Table S2**). This is likely due to variants
282 emerging in blocks (**Figure 2**), though we did observe some mixtures of different lineage groups
283 collected during the transitions between these blocks, e.g. one Delta*-Mu* and three BA.1*-Delta*
284 mixtures (**Figure 6b**, **Table S2**).

285 Since these mixtures have robust sequencing depth (**Figure S12g**) and comprise lineages
286 with as many as 77 discriminating SNPs (**Supplementary Data**), we hypothesized that it would
287 be feasible to resolve lineage haplotypes. Using a standard haplotype phasing tool for long reads
288 (Methods), we were able to produce haplotype blocks in most mixtures (277 or 73.1%), favoring
289 mixtures harboring discriminating SNPs greater in number and closer together (**Figure 6c**). We
290 also developed a custom approach that employs a greedy strategy to merge haplotype blocks
291 together based on the alleles of the discriminating SNPs in each haplotype block (Methods). This
292 greatly increased haplotype block resolution, on average increasing the number of SNPs in the
293 largest (merged) haplotype block by ~100% and increasing the size of haplotype blocks to as long
294 as 15.8kbp (**Figure 6d-e**). These exceptionally large haplotype blocks were found among the
295 BA.1*/Delta* mixtures, which have the largest number of discriminating SNPs among the
296 mixtures identified (**Supplementary Data**). One example is LC0471172, which is a mixture of

297 BA.1.1.18 and AY.39 that had a final merged haplotype block of length 15.8kbp harboring 61 SNPs
298 and spanning most of ORFs 1a and 1b as well as the entire S gene and 3' end of the genome (**Figure**
299 **S14**). These rare, finely resolved mixture haplotypes are evidence that combining haplotype
300 reconstruction with mixture analysis has potential to unveil unique sample characteristics. This
301 mixture analysis workflow thus provides our surveillance apparatus with the essential ability to
302 detect co-infections and ensures that consensus genomes are correctly reported in such cases.

303 **Discussion**

304 Genomic surveillance, globally and through our contribution to CDC SPHERES, proved to be
305 critical for monitoring the emergence of highly mutated SARS-CoV-2 variants and their potential
306 influence on disease severity[38] and the hundreds of vaccine development efforts worldwide (183
307 in clinical development as of March 30, 2023[39]). In this report we showcased our robust,
308 comprehensive U.S.-based SARS-CoV-2 surveillance network enabled through our infrastructure
309 and sequencing capabilities. Our probe-based tiling of the genome precluded surveillance
310 interruptions, while other amplicon-based assays have required multiple updates[10]. However,
311 while our tiled approach has ensured robust lineage detection so far, there is always a possibility
312 that an emerging novel lineage may introduce mutations that could potentially affect our ability to
313 detect it. To address this uncertainty we routinely assess emerging SARS-CoV-2 lineages using
314 our Virseq assay simulator before they are widely circulating among the U.S. population. These
315 resources ensure that we are prepared to swiftly respond to any sudden and/or large mutations in
316 the SARS-CoV-2 genome.

317 One key feature of our surveillance network is the rapid sequestration and consolidation of
318 high viral titer samples before sequencing. This strategy could in theory be applied to any

319 infectious agent for which we or others have robust diagnostic assays. In the case of SARS-CoV-
320 2 in this study we apply an N1 Ct value upper limit for sample inclusion to guarantee sufficient
321 genetic material for whole genome sequencing. While necessary for sequencing feasibility, this
322 thresholding may introduce bias in the sample selection and comprehensive lineage coverage.
323 Another important aspect of our surveillance is the dense network of various Labcorp® testing
324 centers throughout the U.S. In this study we that show our SARS-CoV-2 diagnostic samples come
325 from all HHS regions and are sent for whole genome sequencing through our Virseq assay with
326 limited bias. Importantly, this comprehensive demographic coverage is contingent on the
327 availability of samples from our testing centers, which could potentially change due to myriad
328 factors such as local mandates and/or health care coverage.

329 Our targeted long-read sequencing approach is also equipped for recovery of haplotype-
330 resolved viral genomes. To our knowledge, our study is the first to provide a pandemic-wide, high-
331 resolution evaluation of co-infections at this scale, though there have been other systematic efforts
332 that are smaller[40] or target specific types of co-infections, e.g. Omicron/Delta[37]. A crucial step in
333 confirming co-infections is the haplotype phasing of observed heterozygous mutations, which is
334 generally limited to long-read sequencing approaches described here with PacBio® sequencing and
335 by others using Oxford Nanopore Technologies®[41]. In our study we observe most co-infections
336 from the same lineage group (e.g. BA.1*/BA.1*), likely representing individuals who were
337 exposed to unique variants in rapid succession rather than those who are chronically ill from a
338 previous infection. These co-infections may not only have clinical relevance[30], but also represent
339 potential recombination events. For example, the BA.1 wave showed the highest prevalence of co-
340 infections in our dataset and incidentally introduced numerous recombinants, including those
341 formed from Delta and BA.1[42–44]. Ultimately, the use of long reads is uniquely suited for

342 distinguishing co-infections from these recombinant cases as well as other sources of intra-host
343 variation of the virus that have been described[31].

344 The surveillance apparatus we describe is not only robust to the pandemic undulations but
345 is also flexible and modular. For example, we recently adapted this workflow to employ an Oxford
346 Nanopore Technologies®-based ClearLabs® sequencing approach in lieu of our probe-based long-
347 read (PacBio®-based) sequencing approach. This alternative EUA approved pipeline enables rapid
348 turnaround time (~1 day) and retains the same suite of analytical tools as our primary surveillance
349 apparatus. We have also leveraged our infrastructure to provide additional features beyond
350 monitoring SARS-CoV-2 genetic evolution. Early in the COVID-19 pandemic it became clear that
351 convalescent sera from COVID-19 survivors would be essential for development of antibody
352 therapies[45]. We and others analyzed sera specimens collected from over 3,000 unvaccinated
353 individuals and found that most did not exceed antibody concentrations associated with 90%
354 vaccine efficacy, indicating that vaccination is necessary for maximum protection against SARS-
355 CoV-2 infection[46]. We also use our infrastructure to systematically obtain sera from individuals
356 recently infected with SARS-CoV-2 VOCs as part of multiple efforts to investigate antibody cross-
357 reactivity, which is essential for development of COVID-19 vaccine boosters.

358 As the threat of COVID-19 wanes and global SARS-CoV-2 surveillance networks scale
359 back, there is a strong need for continued development of rapid response tools. Diagnostics that
360 target multiple pathogens, such as our seasonal respiratory panel[47], are increasingly useful to this
361 end. These diagnostics may serve as outbreak detection tools when their negativity rate spikes,
362 indicating the emergence of a novel pathogen. Agnostic surveillance techniques, such as those
363 monitoring wastewater via shotgun sequencing[13–15,17], have already shown promise by detecting
364 Poliovirus Type 2 in New York wastewater[48]. If an outbreak does not immediately attenuate, then

365 our surveillance apparatus described in this study could serve as a model for sustained monitoring
366 of whole genome variations that could impact disease severity, outbreak dynamics, and the
367 efficiency of targeted diagnostic assays.

368 In this retrospective study, we showcase our unique positioning for rapid development and
369 maintenance of robust pathogen surveillance. Our nationwide surveillance network and its suite of
370 analytical and sequencing components collectively serve as a model for future large-scale
371 surveillance efforts. Looking to the future, it is our mission to stay vigilant and continue refining
372 this model to combat the many emergent infectious diseases posing imminent threats to public
373 health.

374 **Methods**

375 ***Ethical Statement***

376 The use of residual de-identified samples for this study was determined as not a human subject
377 research requiring IRB review.

378 ***SARS-CoV-2 surveillance and whole genome sequencing***

379 Extracted total nucleic acid from positive specimens identified through the Labcorp® FDA EUA
380 approved COVID-19 RT-PCR Test or SARS-CoV-2 & Influenza A/B Assay Test were sequestered
381 and consolidated using a Hamilton Microlab® STAR™ instrument and plate selector app, retaining
382 only positive samples with N1 Ct values less than 31. Sample RNA was reverse transcribed to
383 cDNA and a specially designed SARS-CoV-2 probe set containing ~1000 tiled Molecular Loop®
384 Loopcap™ Molecular Inversion Probes (MIPS) was used to amplify the cDNA from 99.6% of the
385 SARS-CoV-2 genome with most bases covered by 22 MIPs[19]. The product synthesized in-between

386 the MIPs was enriched and had sample specific molecular barcodes added via amplification for
387 long-read sequencing on a Pacific Biosciences® Sequel II™[49].

388 ***Sequence quality control and post-processing***

389 After sequencing, circular consensus sequence (CCS) bam files were generated using the PacBio®
390 SMRT LINK™ software v9.0 ccs program[50] and subsequently demultiplexed using lima with the
391 following parameters: "--min-score-lead -1", "--min-score 80", "--window-size-multi 1.1", "--
392 neighbors". Molecular Loop® barcodes were then trimmed by aligning sequences to barcodes
393 using pbmm2 with parameters "--sort" and "--preset HIFI" and custom processing scripts. Final
394 sample fastq files were generated by converting the resulting bam files using BamTools[51].

395 Sequence fastq files were analyzed using a genome analysis pipeline implemented in the
396 CLC Genomics Server version 9.1.1[52]. This workflow starts with a sample-level fastq file and uses
397 Minimap2[53] to align reads to the SARS-CoV-2 reference genome (NCBI GenBank reference
398 NC_045512.2) to generate a bam file of the alignment as well as a VCF file containing the variants
399 called using a custom variant caller in CLC. A consensus sequence for each sample was then
400 generated using VCFCons v8.5.0[54]. When VCFCons calls a nucleotide sequence for genome
401 construction it was required to have least 4 CCS reads covering that base pair and an alternate
402 allele frequency compared to the reference of at least 80%. If the alternate allele frequency was
403 between 20% and 80%, then the appropriate ambiguous IUPAC nucleotide was called. If a
404 nucleotide was covered by less than 4 CCS reads it was reported as ambiguous (N) in the consensus
405 sequence.

406 Three different coverage quality control metrics were used to ensure high accuracy of
407 resulting consensus genome sequences. Firstly, the median CCS read coverage was calculated
408 separately for 29 ~1kb genomic regions and each sample was required to have at minimum 10X

409 mean of median amplicon coverage (depth of coverage). For samples to be kept for downstream
410 Phylogenetic Assignment of Named Global Outbreak (PANGO) lineage determination[18] and
411 sequence analysis, a minimum genome coverage of 50% was required. For sample genome
412 sequences to be reported to the CDC (and later deposited to GISAID[20]), a more stringent genome
413 coverage threshold of 90% was applied along with a third coverage filter that required no more
414 than 1 ambiguous base call in each 6bp sliding window of the S gene. Furthermore, samples were
415 reported within 21 days of collection.

416 Sample consensus genome sequences with at least 10X depth of coverage and genome
417 coverage of at least 50% were further analyzed using pangolin software[29] (v4.3.1 with pangolin
418 data v1.22) and the UShER algorithm[55] with default parameters to determine SARS-CoV-2
419 PANGO lineages. Sequences and their mutations were also characterized using Nextclade
420 v2.14.0[56] and the Nextclade SARS-CoV-2 dataset compiled on August 9th, 2023. In all subsequent
421 analyses, PANGO lineages were assigned groups by a pre-determined set of parent lineages,
422 representing key variants of concern (VOCs) throughout the pandemic. A lineage and its
423 descendants are indicated by appending "*". When a lineage is a descendant of two of the
424 following parent lineage groups, the closest parent was selected. If a lineage was not a descendant
425 of any of the parents, then it was placed in the "other" group. Parent lineage groups are as follows:
426 Alpha (B.1.1.7*), Beta (B.1.351*), Gamma (P.1*), Epsilon (B.1.427* and B.1.429*), Eta
427 (B.1.525*), Iota (B.1.526*), Kappa (B.1.617.1*), Mu (B.1.621*), Zeta (P.2*), Delta (B.1.617.2*),
428 BA.1*, BA.2*, BA.4*, BA.5*, BQ*, XBB*, XBB.1.5*, XBB.1.9*, and XBB.1.16*.

429 ***Demographic and phylogenetic analysis***

430 Time-resolved phylogenetic analysis of SARS-CoV-2 consensus genome sequences was
431 performed using augur v.22.2.0[57] and auspice.us v0.12.0 (Auspice 2.49.0) within the Nextstrain

432 framework[58]. Consensus genomes were restricted to those with 100% S gene coverage and at least
433 99% genome coverage sequenced between January 2021 and June 2023. The augur filter utility
434 was used to limit the dataset to a maximum of 1,000 sequences per month each with metadata
435 including sample collection date and PANGO lineage. Next, the augur refine utility was used to
436 create a time-resolved phylogenetic tree using the TreeTime algorithm[59]. Finally, the resulting tree
437 was annotated with lineage information using the augur export utility, and the final tree was
438 displayed on auspice.us.

439 Age and gender distributions of all samples in this study with consensus genomes passing
440 the minimal coverage criteria for PANGO lineage determination were analyzed, restricting to those
441 collected between January 2021 and June 2023 with weekly sample counts of at least 100.
442 Distributions were also stratified by U.S. HHS regions[60]. For each region, annual gender
443 proportions were calculated, and age distributions were determined by aggregating ages into
444 different groups as follows: 0-17 (pediatrics), 18-19, 20-29, 30-39, 40-49, 50-59, 60-69, 70-79,
445 and 80 or older.

446 ***RT-PCR sampling, positivity, and N1 Ct value analysis***

447 Demographic data and positive/negative results of RT-PCR samples collected through the
448 surveillance network described in this study were aggregated for multiple analyses. First, the RT-
449 PCR sampling was compared with Virseq assay sampling across each HHS region and month
450 where at least 100 Virseq samples were sequenced. The geographic distribution of RT-PCR and
451 Virseq sampling were also independently assessed by normalizing with U.S. state census data from
452 2020-2022[61]. Census data from 2023 was estimated by averaging that from 2020-2022. Overall
453 RT-PCR positivity was analyzed weekly and was also stratified by gender and age groups
454 (described in Methods section 'Demographic and phylogenetic analysis'). N1 Ct values of Virseq

455 samples were analyzed weekly and stratified based on whether samples were collected before or
456 after the Omicron wave (November 2021 to February 2022), denoted as 'pre-wave', 'Omicron
457 wave', and 'post-wave'. N1 Ct values were also compared based on co-infection status using only
458 deeply sequenced samples from the co-infection analysis described later in Methods section
459 'Workflow for detection and characterization of SARS-CoV-2 mixtures'.

460 ***Whole genome coverage and mutation frequency analysis***

461 Genome-wide assessment of SARS-CoV-2 sequence mutation frequencies was performed using
462 all results obtained from Nextclade v2.14.0[56] for samples passing minimal coverage quality
463 control. Mutations were considered as "lineage-defining" if they appeared in at least 70% of the
464 genome sequences assigned to that lineage. The number of mutations with at least 5% prevalence
465 across the entire genome and within specific SARS-CoV-2 genic regions was calculated for each
466 sample collection week. Circulating lineage diversity was calculated in each week using unique
467 lineage counts and the Shannon entropy implementation in the vegan R package[62]. In all analyses
468 that indicate dominant lineage groups during specific time periods, this was calculated using the
469 first week where at least 5% of the lineages were assigned to that lineage group. In the case of
470 XBB.1.9 and XBB.1.16, these were combined, and the sum of their occurrences was used.

471 Per-base CCS coverage analysis was performed using selected VOCs (B.1.1.7, B.1.617.2,
472 BA.1, BA.2, BA.4, BA.5, BQ.1, and XBB.1.5), where the sequences chosen were required to have
473 depth of coverages of 100 +/- 10. 50 sequences were randomly chosen for each VOC that met the
474 coverage constraint and had the exact PANGO lineage determination of the VOC. Per-base
475 coverage was determined using Samtools[63] depth with parameters "-q 0 -Q 0" applied to the sample
476 alignment bam files. Median per-base coverage was then calculated for each VOC and smoothed
477 using a 30bp sliding window. Lineage defining mutation density was also determined for each

478 VOC by enumerating mutations at each genomic position and smoothing over a 1kbp sliding
479 window.

480 ***Virseq performance simulator***

481 The Virseq pipeline performance was assessed by constructing a process whereby an input whole
482 genome sequence is mutated in a manner that simulates the coverage and errors introduced by
483 sequencing and post-processing analysis. This simulator was constructed using coverage and error
484 models of a representative sequencing batch selected from February 2022 containing 520 samples
485 reported to CDC (**Supplementary Data**). The coverage model was designed using a min max
486 normalization strategy, where two components were stored for later application of the model: 1) a
487 list of each sample's maximum per-base coverage and 2) the mean min max normalized coverage
488 at each position of the genome. In practice, since the peripheral 5' and 3' ends of the genome do
489 not have tiled coverage by design, a sample's min max normalized coverages equate to positional
490 coverage divided by the maximum per-base coverage. The error model was generated under the
491 assumption that the consensus at each base position is the correct base call. Thus, the probability
492 of an error was calculated using the maximum minor allele frequency. At each genomic position
493 the number of each base call was enumerated in R using Rsamtools[64] to identify the error rates for
494 each sample, and the mean error rate at each position was recorded. If the median coverage at a
495 position was less than 3, then the global median error rate was used. If the error rate was zero (i.e.
496 there were not any alternate base calls at a position), then half of the global minimum non-zero
497 error rate was used instead.

498 These two models were collectively applied to an input SARS-CoV-2 whole genome
499 sequence first by identifying positional coverages. A maximum coverage was randomly selected
500 from the list obtained from the representative batch and the expected mean coverage was computed

501 at each position by multiplying this maximum coverage by each pre-computed mean positional
502 fractional coverage. Next, the coverage at a position was sampled from a Poisson distribution using
503 the mean obtained in the prior step. If the sampled coverage was less than the minimum per-base
504 coverage threshold of 4, then an ambiguous base call was simulated at that position (see Methods
505 section 'Sequence quality control and post-processing'). Next, for all remaining unambiguous
506 positions a consensus base call was simulated using the sampled coverage and the pre-computed
507 average error at each position. Bases were sampled using a cumulative binomial using the average
508 error and coverage, and if the number of errors exceeded half of the base calls a random base was
509 called at the position; otherwise, the reference base was used. Finally, the PANGO lineages were
510 determined for both the original and simulated sequence using pangolin software[29] (v4.3.1 with
511 pangolin data v1.22) and checked for concordance. If the lineages were identical, the result was
512 considered an 'exact match'. If one lineage was a descendant of the other, then the result was
513 categorized as a 'parent match'. All other cases were considered 'discordant'.

514 Two simulation experiments were used to assess the performance of the Virseq pipeline.
515 Sequences were retrieved from GISAID[20] (accessed August 25th, 2023) and those used in the
516 experiments were restricted to those with at least 99% genome coverage, ensuring high quality
517 lineage calls. The first experiment assessed up to 100 sequences from each VOC and descendant
518 lineages thereof, current and former, designated in pangolin data v1.22. The second experiment
519 used a random selection of 10,000 sequences from each month ranging from January 2021 to July
520 2023.

521 ***Workflow for detection and characterization of SARS-CoV-2 mixtures***

522 A custom workflow was developed to detect and characterize samples containing more than one
523 unique PANGO lineage, i.e. mixtures or co-infections. All bam files of samples passing minimum

524 coverage metrics were processed through the recommended freyja[14] processing workflow, first
525 calling variants using iVar[65] and subsequently using the freyja demixing algorithm[14] to determine
526 the lineage abundances in each sample. This algorithm attempts to identify a parsimonious set of
527 lineages best explaining the UShER[55] defining single nucleotide polymorphisms (SNPs) detected
528 in the sample.

529 Lineage abundances were then processed, greedily aggregating abundances of lineages
530 with parent/descendant relationships (e.g. BA.1 and BA.1.1) starting with the most abundant
531 lineage. This was performed since one lineage would have UShER[55] defining SNPs forming a
532 subset or superset of the other lineage, and it was assumed that this splitting of highly similar
533 lineages was due to sequencing noise. Samples were then filtered, requiring an empirically
534 determined minimum depth of coverage where the rate of mixture detection was stable and low
535 (**Supplementary Figure 12a**). Mixtures were then required to satisfy three criteria: 1) Top lineage
536 relative abundance no greater than 0.8, 2) second lineage relative abundance no less than 0.2, and
537 3) minimum of 3 UShER[55] defining SNPs discriminating the two lineages comprising the mixture
538 (**Supplementary Figure 12b-f**). Each resulting mixture sample was then categorized using the
539 parent lineage groups of the two mixed lineages (see Methods section 'Sequence quality control
540 and post-processing').

541 Mixture samples were then processed using WhatsHap[66], a standard haplotype assembly
542 tool suitable for long sequencing reads. If a sample did not yield any haplotype blocks (i.e. no two
543 SNPs were phased), then analysis was halted. If only a single haplotype block was obtained, then
544 the block length and phased mutations therein were recorded. If a sample had at least two haplotype
545 blocks, then a greedy algorithm was applied to merge these blocks while leveraging *a priori*
546 mixture knowledge yielded by freyja[14]. The number of UShER[55] defining SNPs unique to each

547 mixture lineage (i.e. lineage-discriminating SNPs) was recorded for each block, and blocks were
548 iteratively merged in order of descending number of lineage-discriminating SNPs (ties broken by
549 using the larger block length). Blocks were merged to maximize the number of correctly phased
550 lineage-discriminating SNPs. If the addition of a block to this greedily merged block didn't
551 improve this optimization criterion, then it was skipped, and the next block was assessed. This
552 process continued until no further blocks with lineage-discriminating SNPs remained. A custom
553 script was used to modify the haplotagged bam output by WhatsHap[66] for visualization of merged
554 haplotype blocks in Integrative Genomics Viewer v2.16.2[67].

555 **Author Contributions**

556 Development and maintenance of Virseq surveillance apparatus – all authors. Manuscript
557 supervision and administration – L.K.I. Manuscript conceptualization and methodology – H.N.B.,
558 K.S., Q.Zh., J.D.W., S.L., and L.K.I. Formal analysis and data curation – H.N.B. and K.S. Formal
559 analysis review – H.N.B., K.S., Q.Zh., S.L., and L.K.I. Preparation of manuscript figures and
560 tables – H.N.B. and K.S. Original manuscript draft preparation – H.N.B. Manuscript review and
561 editing – H.N.B., K.S., Q.Zh., Q.Ze., J.D.W., M.B.N., S.E.D., J.Me., M.E., S.L., and L.K.I.
562 Approval of final manuscript – all authors.

563 **Funding Statement**

564 No grants or financial support were used for this study.

565 **Acknowledgements**

566 We would like to acknowledge the dedicated members of our IT infrastructure team who continue
567 to be instrumental in maintaining the resources needed for this surveillance effort. We would also

like to thank the hundreds of technicians and technologists who processed SARS-CoV-2 PCR testing at Labcorp during the pandemic. Without the hard work and dedication of the broader Labcorp enterprise, this surveillance effort would not have been possible. We would also like to extend our gratitude to the dedicated teams at PacBio and Molecular Loop who were instrumental in helping us set up their respective resources for use in the Virseq pipeline. We would especially like to thank Elizabeth Tseng at PacBio for her significant contribution towards the development of the VCFCons software used in the Virseq pipeline. Lastly, we would like to thank the U.S. Centers for Disease Control (CDC) for their guidance throughout this surveillance effort.

Competing Interests

All authors (except O.C.) are employees of Labcorp, a provider of clinical diagnostic services. O.C. is a former Labcorp employee and is now employed by Fortrea, Inc.

Data Availability

Figures S1-13 and **Table S1** may be found in the **Supplementary Materials**. A list of de-identified LCIDs and their corresponding GISAID EPI_ISL IDs from samples analyzed in this study that were reported to CDC may be found in the **Supplementary Data**. A list of LCIDs used to construct the empirical simulation model are included in the **Supplementary Data**. Additionally, all processed data used to generate **Figures 2b**, **3b**, **4-6**, and **S1-13** are provided in the **Supplementary Data**. Data used to generate **Figure 3a** are provided in **Table S1**.

References

1. Wu, F. *et al.* A new coronavirus associated with human respiratory disease in China. *Nature* **579**, 265–269 (2020).

589 2. Lu, R. *et al.* Genomic characterisation and epidemiology of 2019 novel coronavirus:
590 implications for virus origins and receptor binding. *The Lancet* **395**, 565–574 (2020).
591 3. Zhou, P. *et al.* A pneumonia outbreak associated with a new coronavirus of probable bat
592 origin. *Nature* **579**, 270–273 (2020).
593 4. Cohen, O. *et al.* Labcorp's perspective: Responding to SARS-CoV-2 and the next pandemic.
594 *Nat. Portf.* (2022).
595 5. Sullivan, A. *et al.* Follow-Up SARS-CoV-2 PCR Testing Outcomes From a Large Reference
596 Lab in the US. *Front. Public Health* **9**, 679012 (2021).
597 6. Sullivan, A. *et al.* Antibody titer levels and the effect on subsequent SARS-CoV-2 infection
598 in a large US-based cohort. *Heliyon* **9**, e13103 (2023).
599 7. Alfego, D. *et al.* A population-based analysis of the longevity of SARS-CoV-2 antibody
600 seropositivity in the United States. *EClinicalMedicine* **36**, 100902 (2021).
601 8. Markov, P. V. *et al.* The evolution of SARS-CoV-2. *Nat. Rev. Microbiol.* **21**, 361–379 (2023).
602 9. Tao, K. *et al.* The biological and clinical significance of emerging SARS-CoV-2 variants.
603 *Nat. Rev. Genet.* **22**, 757–773 (2021).
604 10. Itokawa, K., Sekizuka, T., Hashino, M., Tanaka, R. & Kuroda, M. Disentangling primer
605 interactions improves SARS-CoV-2 genome sequencing by multiplex tiling PCR. *PLOS*
606 *ONE* **15**, e0239403 (2020).
607 11. Vacca, D. *et al.* Direct RNA Nanopore Sequencing of SARS-CoV-2 Extracted from Critical
608 Material from Swabs. *Life Basel Switz.* **12**, 69 (2022).
609 12. Rehn, A. *et al.* Catching SARS-CoV-2 by Sequence Hybridization: a Comparative Analysis.
610 *mSystems* **6**, e0039221 (2021).

611 13. Baaijens, J. A. *et al.* Lineage abundance estimation for SARS-CoV-2 in wastewater using
612 transcriptome quantification techniques. *Genome Biol.* **23**, 236 (2022).
613 14. Karthikeyan, S. *et al.* Wastewater sequencing reveals early cryptic SARS-CoV-2 variant
614 transmission. *Nature* **609**, 101–108 (2022).
615 15. Smyth, D. S. *et al.* Tracking cryptic SARS-CoV-2 lineages detected in NYC wastewater. *Nat.*
616 *Commun.* **13**, 635 (2022).
617 16. Wang, X. *et al.* Fecal viral shedding in COVID-19 patients: Clinical significance, viral load
618 dynamics and survival analysis. *Virus Res.* **289**, 198147 (2020).
619 17. Kitajima, M. *et al.* SARS-CoV-2 in wastewater: State of the knowledge and research needs.
620 *Sci. Total Environ.* **739**, 139076 (2020).
621 18. O'Toole, Á., Pybus, O. G., Abram, M. E., Kelly, E. J. & Rambaut, A. Pango lineage
622 designation and assignment using SARS-CoV-2 spike gene nucleotide sequences. *BMC*
623 *Genomics* **23**, 121 (2022).
624 19. LoopCap™ Technology Elegant, High-Performance Targeted NGS.
625 https://molecularloop.com/wp-content/uploads/2023/04/Molecular-Loop-Tech-
626 Note_0423_Final.pdf (2023).
627 20. Elbe, S. & Buckland-Merrett, G. Data, disease and diplomacy: GISAID's innovative
628 contribution to global health. *Glob. Chall. Hoboken NJ* **1**, 33–46 (2017).
629 21. Sayers, E. W. *et al.* Database resources of the national center for biotechnology information.
630 *Nucleic Acids Res.* **50**, D20–D26 (2022).
631 22. Puhach, O., Meyer, B. & Eckerle, I. SARS-CoV-2 viral load and shedding kinetics. *Nat. Rev.*
632 *Microbiol.* **21**, 147–161 (2023).

633 23. Sentis, C. *et al.* SARS-CoV-2 Omicron Variant, Lineage BA.1, Is Associated with Lower
634 Viral Load in Nasopharyngeal Samples Compared to Delta Variant. *Viruses* **14**, 919 (2022).
635 24. CDC Expands Booster Shot Eligibility and Strengthens Recommendations for 12-17 Year
636 Olds. https://www.cdc.gov/media/releases/2022/s0105-Booster-Shot.html (2022).
637 25. CDC Recommends Pfizer Booster at 5 Months, Additional Primary Dose for Certain
638 Immunocompromised Children. https://www.cdc.gov/media/releases/2022/s0104-Pfizer-
639 Booster.html (2022).
640 26. Coronavirus (COVID-19) Update: FDA Expands Eligibility for Pfizer-BioNTech COVID-
641 19 Vaccine Booster Dose to Children 5 through 11 Years. https://www.fda.gov/news-
642 events/press-announcements/coronavirus-covid-19-update-fda-expands-eligibility-pfizer-
643 biontech-covid-19-vaccine-booster-dose (2022).
644 27. McMillen, T., Jani, K., Robilotti, E. V., Kamboj, M. & Babady, N. E. The spike gene target
645 failure (SGTF) genomic signature is highly accurate for the identification of Alpha and
646 Omicron SARS-CoV-2 variants. *Sci. Rep.* **12**, 18968 (2022).
647 28. Gayvert, K. *et al.* Evolutionary trajectory of SARS-CoV-2 genome shifts during widespread
648 vaccination and emergence of Omicron variant. *Npj Viruses* **1**, 5 (2023).
649 29. O'Toole, Á. *et al.* Assignment of epidemiological lineages in an emerging pandemic using
650 the pangolin tool. *Virus Evol.* **7**, veab064 (2021).
651 30. Pedro, N. *et al.* Dynamics of a Dual SARS-CoV-2 Lineage Co-Infection on a Prolonged Viral
652 Shedding COVID-19 Case: Insights into Clinical Severity and Disease Duration.
653 *Microorganisms* **9**, 300 (2021).
654 31. Lythgoe, K. A. *et al.* SARS-CoV-2 within-host diversity and transmission. *Science* **372**,
655 eabg0821 (2021).

656 32. Wawina-Bokalanga, T. *et al.* Genomic evidence of co-identification with Omicron and Delta
657 SARS-CoV-2 variants: a report of two cases. *Int. J. Infect. Dis.* **122**, 212–214 (2022).
658 33. Combes, P. *et al.* Evidence of co-infections during Delta and Omicron SARS-CoV-2 variants
659 co-circulation through prospective screening and sequencing. *Clin. Microbiol. Infect.* **28**,
660 1503.e5-1503.e8 (2022).
661 34. Hosch, S. *et al.* Genomic Surveillance Enables the Identification of Co-infections With
662 Multiple SARS-CoV-2 Lineages in Equatorial Guinea. *Front. Public Health* **9**, 818401
663 (2022).
664 35. Zhou, H.-Y. *et al.* Genomic evidence for divergent co-infections of co-circulating SARS-
665 CoV-2 lineages. *Comput. Struct. Biotechnol. J.* **20**, 4015–4024 (2022).
666 36. Francisco Jr, R. D. S. *et al.* Pervasive transmission of E484K and emergence of VUI-NP13L
667 with evidence of SARS-CoV-2 co-infection events by two different lineages in Rio Grande
668 do Sul, Brazil. *Virus Res.* **296**, 198345 (2021).
669 37. Rockett, R. J. *et al.* Co-infection with SARS-CoV-2 Omicron and Delta variants revealed by
670 genomic surveillance. *Nat. Commun.* **13**, 2745 (2022).
671 38. Nguyen, N. N., Nguyen, Y. N., Hoang, V. T., Million, M. & Gautret, P. SARS-CoV-2
672 Reinfection and Severity of the Disease: A Systematic Review and Meta-Analysis. *Viruses*
673 **15**, 967 (2023).
674 39. WHO COVID-19 vaccine tracker and landscape.
675 https://www.who.int/publications/m/item/draft-landscape-of-covid-19-candidate-vaccines
676 (2023).

677 40. Peñas-Utrilla, D. *et al.* Systematic genomic analysis of SARS-CoV-2 co-infections
678 throughout the pandemic and segregation of the strains involved. *Genome Med.* **15**, 57
679 (2023).
680 41. Li, Y. *et al.* Both simulation and sequencing data reveal coinfections with multiple SARS-
681 CoV-2 variants in the COVID-19 pandemic. *Comput. Struct. Biotechnol. J.* **20**, 1389–1401
682 (2022).
683 42. Arora, P. *et al.* The SARS-CoV-2 Delta-Omicron Recombinant Lineage (XD) Exhibits
684 Immune-Escape Properties Similar to the Omicron (BA.1) Variant. *Int. J. Mol. Sci.* **23**, 14057
685 (2022).
686 43. Lacek, K. A. *et al.* SARS-CoV-2 Delta–Omicron Recombinant Viruses, United States.
687 *Emerg. Infect. Dis.* **28**, 1442–1445 (2022).
688 44. Mohapatra, R. K., Kandi, V., Tuli, H. S., Chakraborty, C. & Dhama, K. The recombinant
689 variants of SARS-CoV-2: Concerns continues amid COVID-19 pandemic. *J. Med. Virol.* **94**,
690 3506–3508 (2022).
691 45. Casadevall, A. & Pirofski, L. The convalescent sera option for containing COVID-19. *J. Clin.*
692 *Invest.* **130**, 1545–1548 (2020).
693 46. Schuh, A. J. *et al.* SARS-CoV-2 Convalescent Sera Binding and Neutralizing Antibody
694 Concentrations Compared with COVID-19 Vaccine Efficacy Estimates against Symptomatic
695 Infection. *Microbiol. Spectr.* **10**, e01247-22 (2022).
696 47. Larkin, H. D. First Nonprescription COVID-19 Test That Also Detects Flu and RSV. *JAMA*
697 **328**, 11 (2022).

698 48. Ryerson, A. B. *et al.* Wastewater Testing and Detection of Poliovirus Type 2 Genetically
699 Linked to Virus Isolated from a Paralytic Polio Case — New York, March 9–October 11,
700 2022. *MMWR Morb. Mortal. Wkly. Rep.* **71**, 1418–1424 (2022).
701 49. Rhoads, A. & Au, K. F. PacBio Sequencing and Its Applications. *Genomics Proteomics*
702 *Bioinformatics* **13**, 278–289 (2015).
703 50. Wenger, A. M. *et al.* Accurate circular consensus long-read sequencing improves variant
704 detection and assembly of a human genome. *Nat. Biotechnol.* **37**, 1155–1162 (2019).
705 51. Barnett, D. W., Garrison, E. K., Quinlan, A. R., Strömberg, M. P. & Marth, G. T. BamTools:
706 a C++ API and toolkit for analyzing and managing BAM files. *Bioinforma. Oxf. Engl.* **27**,
707 1691–1692 (2011).
708 52. Liu, C.-H. & Di, Y. P. Analysis of RNA Sequencing Data Using CLC Genomics Workbench.
709 *Methods Mol. Biol. Clifton NJ* **2102**, 61–113 (2020).
710 53. Li, H. Minimap2: pairwise alignment for nucleotide sequences. *Bioinformatics* **34**, 3094–
711 3100 (2018).
712 54. Tseng, E., Zeng, Q. & Iyer, L. VCFCons: a versatile VCF-based consensus sequence
713 generator for small genomes. *bioRxiv* (2021) doi:10.1101/2021.02.26.433111.
714 55. Turakhia, Y. *et al.* Ultrafast Sample placement on Existing tRees (UShER) enables real-time
715 phylogenetics for the SARS-CoV-2 pandemic. *Nat. Genet.* **53**, 809–816 (2021).
716 56. Aksamentov, I., Roemer, C., Hodcroft, E. & Neher, R. Nextclade: clade assignment, mutation
717 calling and quality control for viral genomes. *J. Open Source Softw.* **6**, 3773 (2021).
718 57. Huddleston, J. *et al.* Augur: a bioinformatics toolkit for phylogenetic analyses of human
719 pathogens. *J. Open Source Softw.* **6**, 2906 (2021).

720 58. Hadfield, J. *et al.* Nextstrain: real-time tracking of pathogen evolution. *Bioinforma. Oxf.*
721 *Engl.* **34**, 4121–4123 (2018).
722 59. Sagulenko, P., Puller, V. & Neher, R. A. TreeTime: Maximum-likelihood phylodynamic
723 analysis. *Virus Evol.* **4**, (2018).
724 60. HHS Regional Offices. https://www.hhs.gov/about/agencies/iea/regional-offices/index.html.
725 (2021).
726 61. U.S. Census Bureau. Annual Population Estimates, 2020-2022.
727 https://www2.census.gov/programs-surveys/popest/datasets/2020-2022/state/totals/NST-
728 EST2022-ALLDATA.csv.
729 62. Oksanen, J. *et al.* vegan: Community Ecology Package. https://CRAN.R-
730 project.org/package=vegan. (2022).
731 63. Li, H. *et al.* The Sequence Alignment/Map format and SAMtools. *Bioinformatics* **25**, 2078–
732 2079 (2009).
733 64. Morgan, M., Pagès, H., Obenchain, V. & Hayden, N. Rsamtools: Binary alignment (BAM),
734 FASTA, variant call (BCF), and tabix file import.
735 https://bioconductor.org/packages/Rsamtools. (2021).
736 65. Grubaugh, N. D. *et al.* An amplicon-based sequencing framework for accurately measuring
737 intrahost virus diversity using PrimalSeq and iVar. *Genome Biol.* **20**, 8 (2019).
738 66. Patterson, M. *et al.* WhatsHap: Weighted Haplotype Assembly for Future-Generation
739 Sequencing Reads. *J. Comput. Biol. J. Comput. Mol. Cell Biol.* **22**, 498–509 (2015).
740 67. Robinson, J. T. *et al.* Integrative genomics viewer. *Nat. Biotechnol.* **29**, 24–26 (2011).

741

742 **Figure Legends**

743 **Figure 1. Journey of a sample from raw nasopharyngeal and nasal swabs to CDC reporting.**
744 **a)** Overview of end-to-end genomic surveillance setup. **b)** Consolidation of positive high viral titer
745 samples. **c)** Probe amplification protocol. **d)** Long read sequencing analysis and bioinformatics
746 workflow to prepare high-quality SARS-CoV-2 genomic sequences with demographic metadata
747 for CDC.

748 **Figure 2. SARS-CoV-2 PANGO lineage analysis of 594,832 high-quality genomes from USA**
749 **samples collected between January 2021 and July 2023.** In each plot samples are grouped and
750 colored by the closest parent listed on the top left. **a)** Time-resolved phylogeny of a subset of
751 samples (n=28,069) clustered based on the oldest collected sample with at most 1,000 samples per
752 month. **b)** SARS-CoV-2 lineage proportions across weeks with at least 100 samples (left y-axis)
753 and the PCR positivity rate (%) indicated by the black line (right y-axis).

754 **Figure 3. U.S. nationwide SARS-CoV-2 genomic surveillance consisting of 594,832 high-**
755 **quality genomes from samples collected between January 2021 and July 2023.** In both panels,
756 the U.S. is divided into 10 Health and Human Services (HHS) regions, each in separate colors. **a)**
757 Each state is notated by its two-letter abbreviation and the shade indicates the number of samples
758 collected. Each region uses a shared color gradient, shown on the right in grayscale with maximum
759 and minimum values of 19,000 and 1,000, respectively. **b)** Line plots showing the ratio of Virseq-
760 generated genomes versus the total SARS-CoV-2-positive RT-PCR samples collected on the log2
761 scale over each sample collection month. January 2021 and July 2023 were excluded, as they each
762 have fewer than 100 Virseq-generated genomes in the dataset analyzed. Vertical black lines denote
763 the start of years 2022 and 2023.

764 **Figure 4. Pandemic-wide trends in SARS-CoV-2 genomic mutations and the robustness of**
765 **whole genome probe-based sequencing. a)** Number of mutations with at least 5% prevalence in
766 the lineage population (black) and circulating lineage shannon diversity (red). **b)** Number of
767 mutations with at least 5% prevalence in the lineage population separated by genic origin. **c)**
768 Heatmap showing the genome-wide probe coverage of the most common lineage in circulation for
769 each collection week with genomic positions shown 5' (bottom) to 3' (top). Probes were considered
770 failures if a deletion, insertion, or >3 SNPs were detected in either probe arm. Large genic regions
771 (ORF1a, ORF1b, S) are indicated by horizontal lines and are labeled on the right. In all panels,
772 results are stratified by sample collection week with vertical bars separating the major waves of
773 the pandemic with the causal variant shown above. Waves are demarcated using the collection
774 week when the causal variant first reached 5% prevalence.

775 **Figure 5. Virseq simulation results.** Exact and parent concordance for the retrospective (**a**) and
776 VOC (**b**) simulation experiments. Retrospective results are shown with exact (red) and parent
777 (blue) concordance as separate lines over the sample collection months analyzed, with years
778 demarcated by vertical lines. VOC results are shown with exact and parent concordance results for
779 each VOC data point with 90% thresholds marked by dashed red lines. VOCs colored black have
780 >90% exact concordance, those colored yellow only have >90% parent concordance, and those
781 colored red are below both concordance thresholds. Vertical gray bars separate the major waves of
782 the pandemic with the causal variant shown above. Waves are demarcated using the collection
783 week when the causal variant first reached 5% prevalence.

784 **Figure 6. Haplotype phasing of SARS-CoV-2 mixture samples (i.e. coinfections). a-b)**
785 Prevalence and number of mixtures in each sample collection week with major pandemic waves
786 demarcated as they were in **Figure 3**. In **(a)**, the weekly average (~0.2%) is shown as a horizontal

dashed red line. In **(b)**, mixtures are colored based on the lineage family of the major and minor mixture components, e.g. BA.1*-Delta indicates a mixture of BA.1 and Delta sublineages with majority BA.1. **c)** Sample-level comparison of the number of and minimum distance between UShER defining mutations that discriminate the two mixture lineages. Samples are colored based on their number of defining mutations phased: >1 phased (black, n=149), 1 phased only with non-defining mutation(s) (yellow, n=128), and 0 phased (red, n=102). **d)** Comparison of sample defining mutation phasing among largest resolved haplotype blocks. Results are compared between original whatshap haplotype blocks and those same haplotype blocks merged using freyja mixture results. **e)** The number of defining mutations phased and the lengths of sample merged haplotype blocks.

TABLES

Table 1. Summary of VOCs with more frequent discordant PANGO lineage calls. Each row shows a lineage with < 90% parent concordance and the most common discordant lineage observed among the simulated sequences.

PANGO lineage	Concordance (%)	Total sequences analyzed	Most common discordant lineage
BA.2.2.1	75.00%	4	BA.1
BA.5.10	60.00%	10	BA.5.2
BQ.1.19	75.00%	4	BQ.1.2
BY.1*	86.67%	15	BA.2.75.7
XB*	55.00%	100	B.1
XBV*	78.57%	14	XBB.1
XP*	85.71%	7	BA.1.1

* BY is the alias of BA.2.75.6. XB, XBV, and XP are the following recombinants, respectively: B.1.634/B.1.631, CR.1/XBB.1, and BA.1.1/BA.2.

803 **Figure 1**

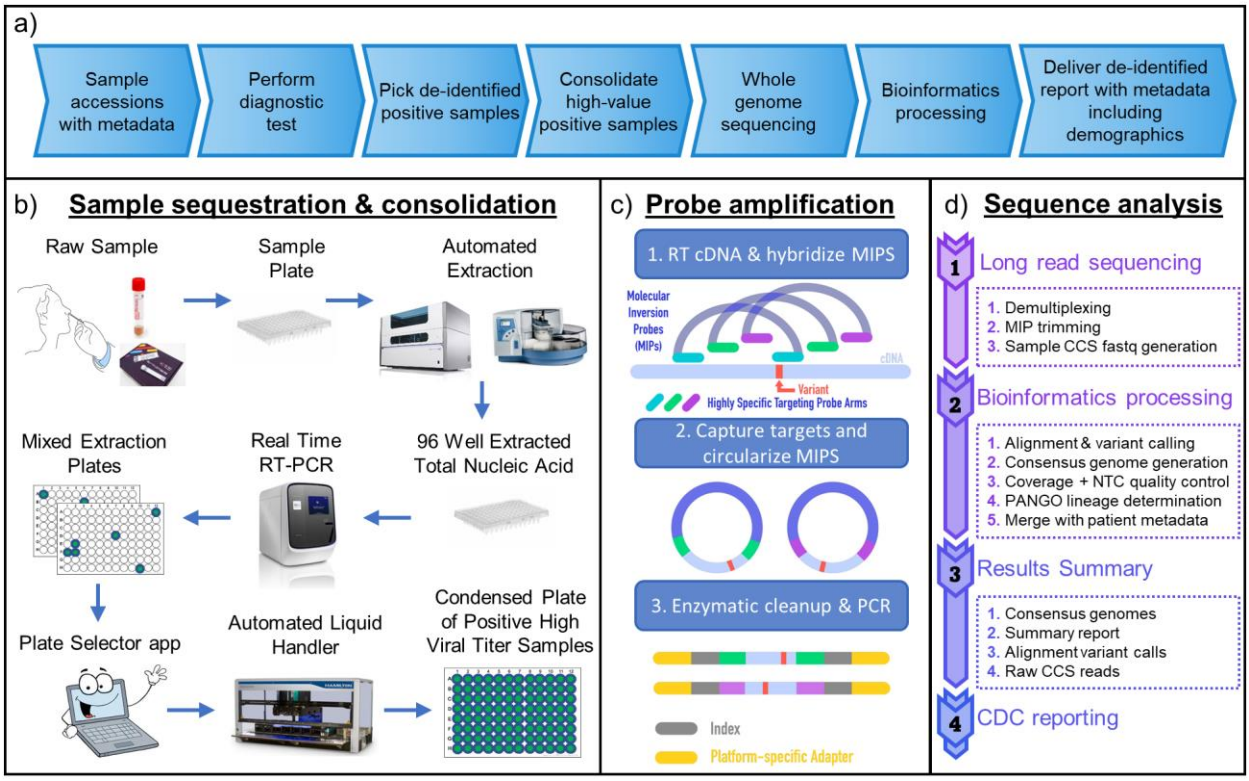

804

Figure 2

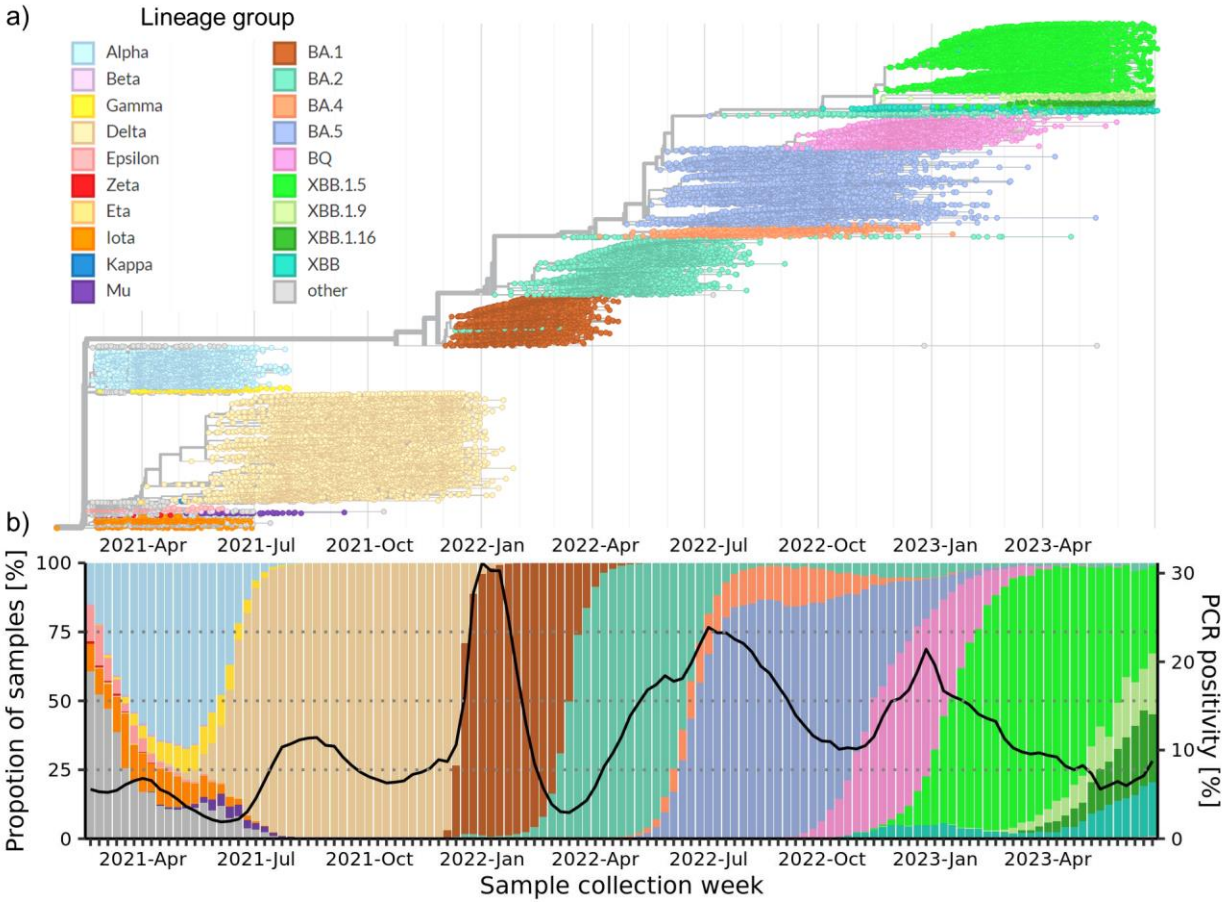
a)
Lineage group
Alpha
Beta
Gamma
Delta
Epsilon
Zeta
Eta
Iota
Kappa
Mu
BA.1
BA.2
BA.4
BA.5
BQ
XBB.1.5
XBB.1.9
XBB.1.16
XBB
other
b)
2021-Apr
2021-Jul
2021-Oct
2022-Jan
2022-Apr
2022-Jul
2022-Oct
2023-Jan
2023-Apr
Propotion of samples [%]
100
75
50
25
0
PCR positivity [%]
30
20
10
0
Sample collection week

807 **Figure 3**

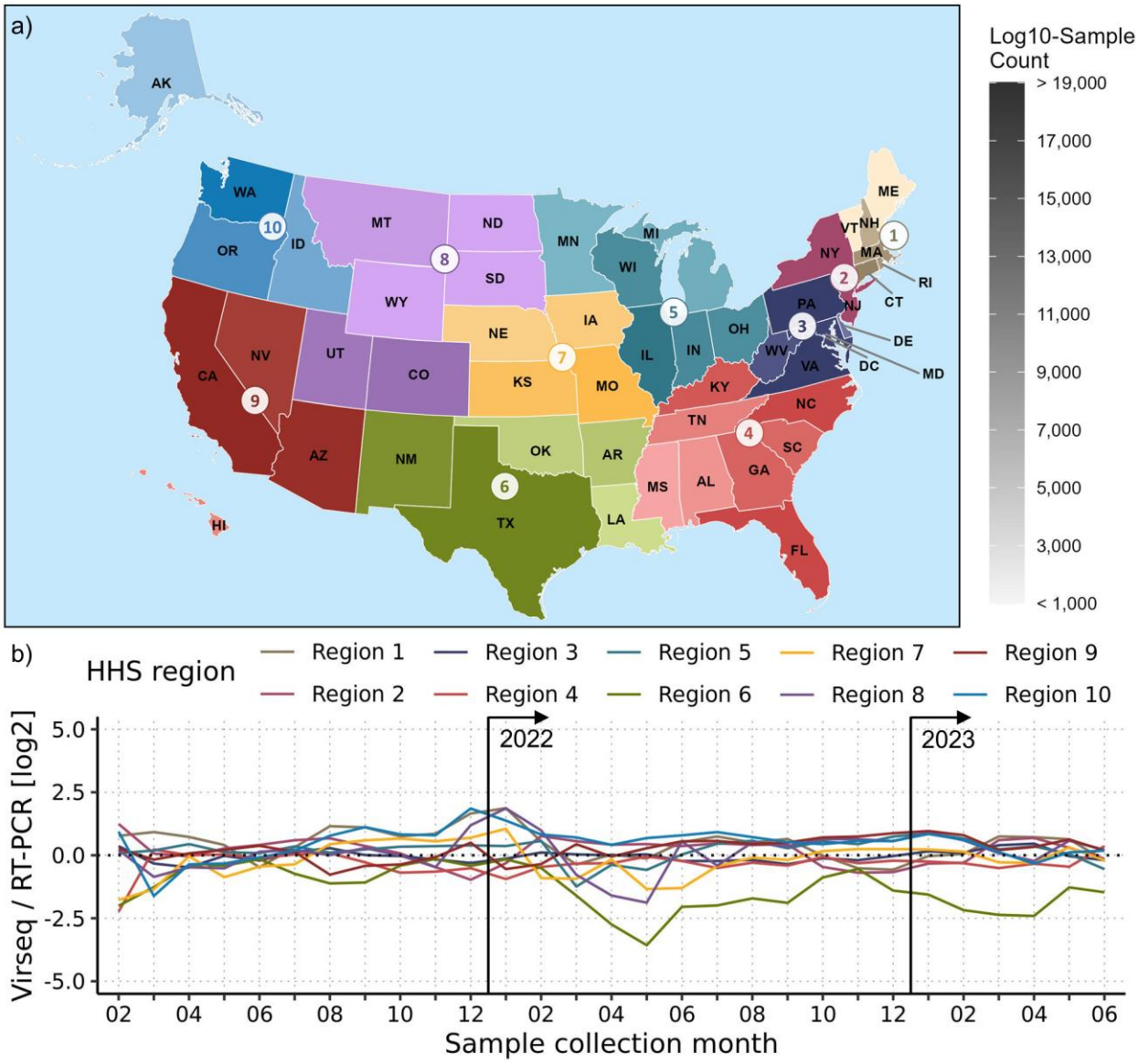

808

Figure 4

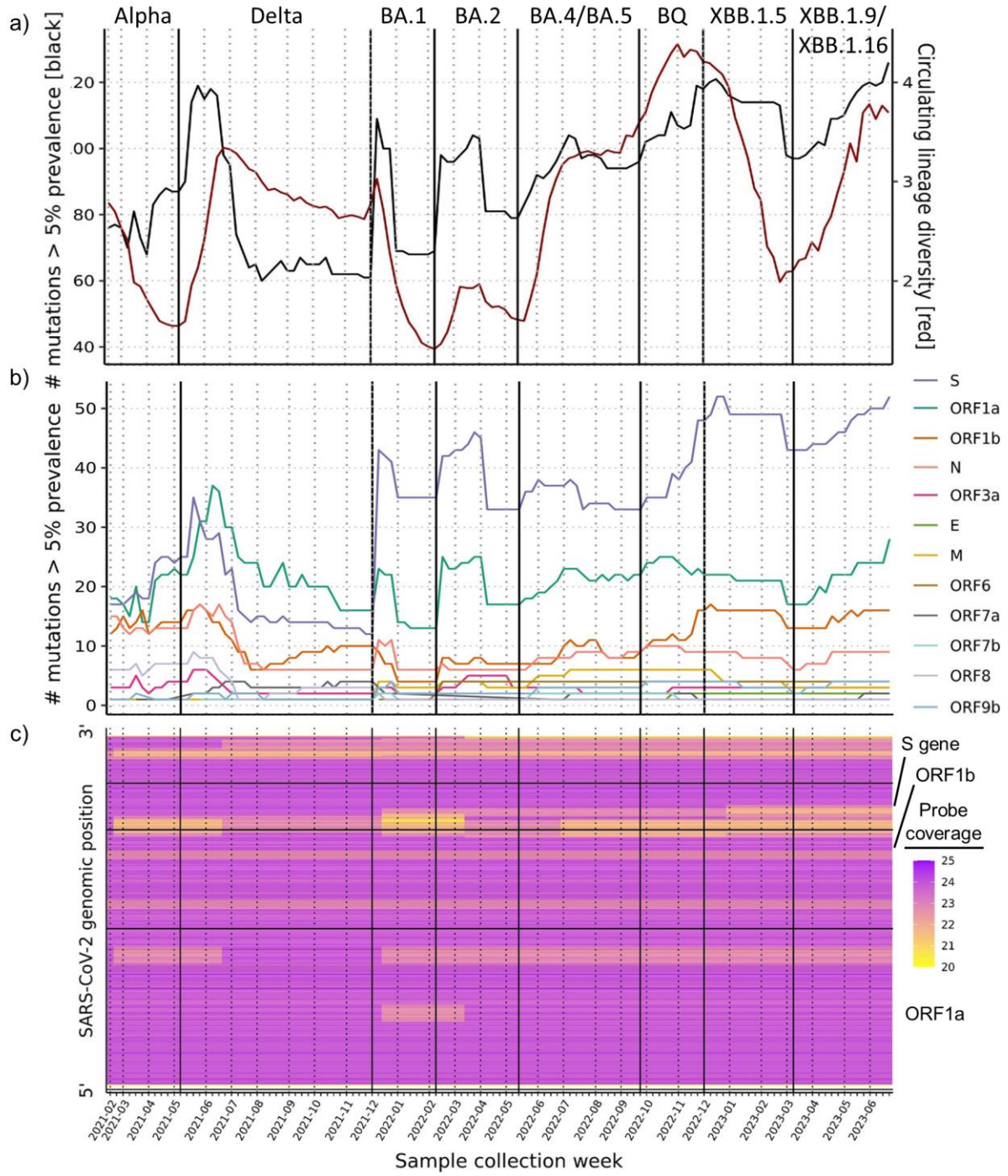
a)
Alpha
Delta
BA.1
BA.2
BA.4/BA.5
BQ
XBB.1.5
XBB.1.9/
XBB.1.16
mutations > 5% prevalence [black]
Circulating lineage diversity [red]
b)
mutations > 5% prevalence
S
ORF1a
ORF1b
N
ORF3a
E
M
ORF6
ORF7a
ORF7b
ORF8
ORF9b
c)
SARS-CoV-2 genomic position
3'
5'
S gene
ORF1b
Probe
coverage
ORF1a
Sample collection week

Figure 5

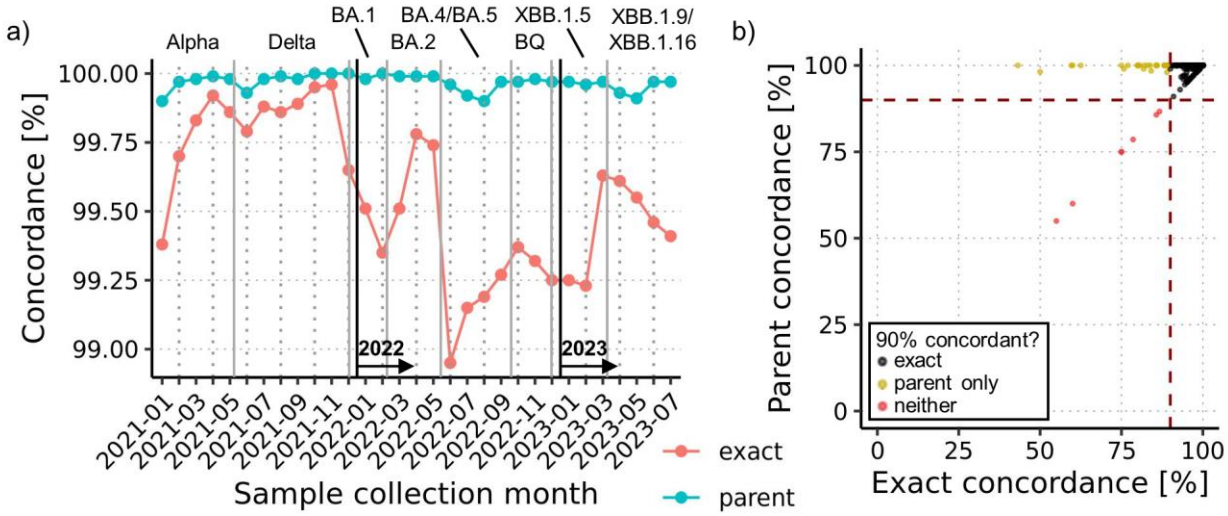
a)
Alpha
Delta
BA.1
BA.4/BA.5
BA.2
XBB.1.5
BQ
XBB.1.9/
XBB.1.16
Concordance [%]
100.00
99.75
99.50
99.25
99.00
2022
2023
2021-01
2021-03
2021-05
2021-07
2021-09
2021-11
2022-01
2022-03
2022-05
2022-07
2022-09
2022-11
2023-01
2023-03
2023-05
2023-07
Sample collection month
exact
parent
b)
Parent concordance [%]
100
75
50
25
0
90% concordant?
exact
parent only
neither
0
25
50
75
100
Exact concordance [%]

Figure 6

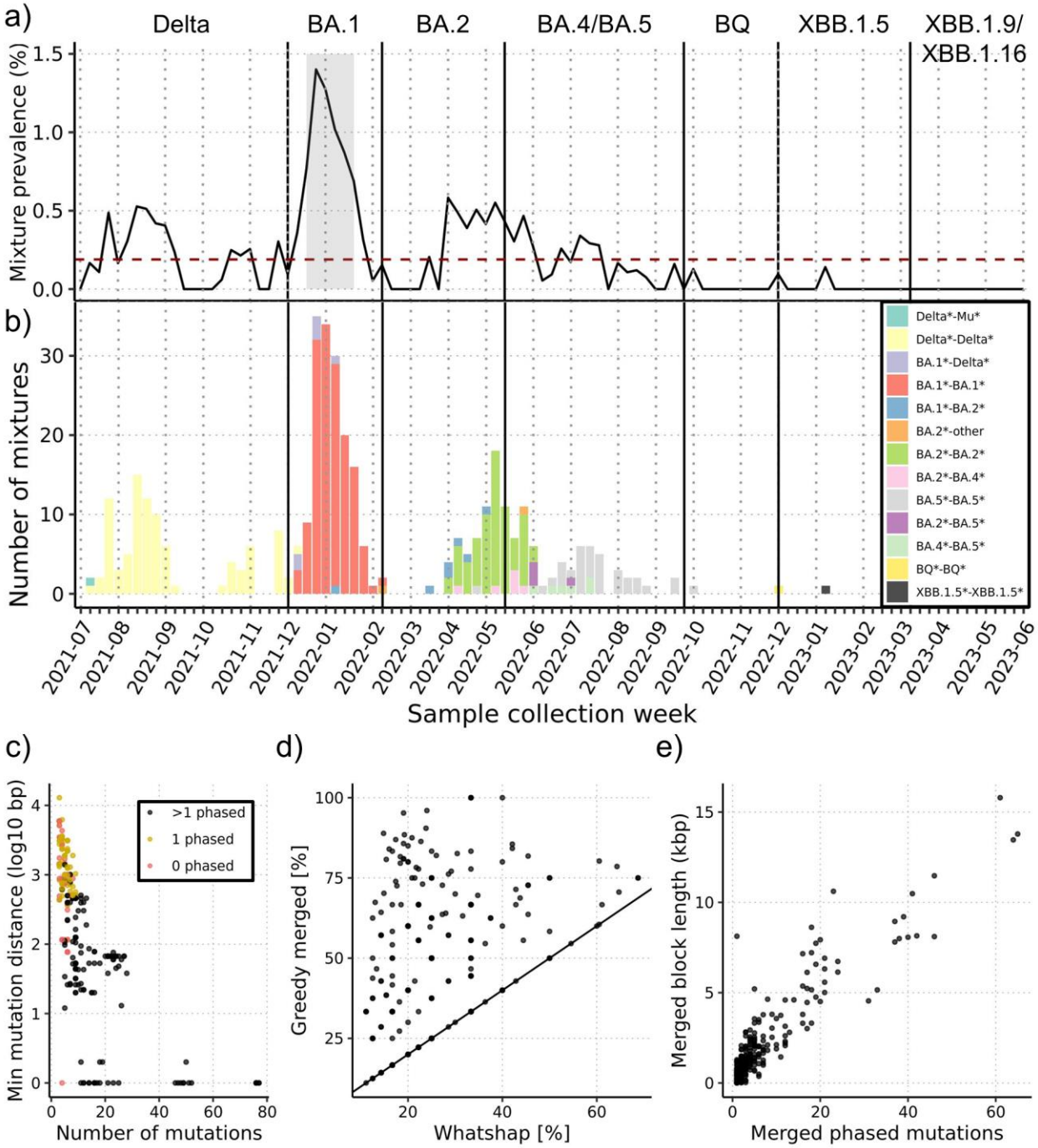
a)
Delta
BA.1
BA.2
BA.4/BA.5
BQ
XBB.1.5
XBB.1.9/
XBB.1.16
Mixture prevalence (%)
b)
Number of mixtures
Delta*-Mu*
Delta*-Delta*
BA.1*-Delta*
BA.1*-BA.1*
BA.1*-BA.2*
BA.2*-other
BA.2*-BA.2*
BA.2*-BA.4*
BA.5*-BA.5*
BA.2*-BA.5*
BA.4*-BA.5*
BQ*-BQ*
XBB.1.5*-XBB.1.5*
Sample collection week
c)
Min mutation distance (log10 bp)
>1 phased
1 phased
0 phased
Number of mutations
d)
Greedy merged [%]
Whatshap [%]
e)
Merged block length (kbp)
Merged phased mutations